

Prosperity before Collapse: How Far Can Off-Policy RL Reach with Stale Data on LLMs?

Haizhong Zheng¹, Jiawei Zhao², Beidi Chen¹

¹Carnegie Mellon University

²Meta AI

{haizhonz, beidic}@cmu.edu, jwzhao@meta.com

Reinforcement learning has been central to recent advances in large language model reasoning, but most algorithms rely on on-policy training that demands fresh rollouts at every update, limiting efficiency and scalability. Asynchronous RL systems alleviate this by decoupling rollout generation from training, yet their effectiveness hinges on tolerating large staleness in rollout data, a setting where existing methods either degrade in performance or collapse. We revisit this challenge and uncover a *prosperity-before-collapse* phenomenon: stale data can be as informative as on-policy data if exploited properly. Building on this insight, we introduce **M2PO** (Second-Moment Trust Policy Optimization), which constrains the second moment of importance weights to suppress only extreme outliers while preserving informative updates. Notably, M2PO sharply reduces the fraction of clipped tokens under high staleness (from 1.22% to 0.06% over training), precisely masking high-variance tokens while maintaining stable optimization. Extensive evaluation across six models (from 1.7B to 32B) and eight benchmarks shows that M2PO delivers stable off-policy training even with data stale by *at least 256 model updates* and matches on-policy performance.



Github: <https://github.com/Infini-AI-Lab/M2PO/>

Website: <https://infini-ai-lab.github.io/M2PO/>

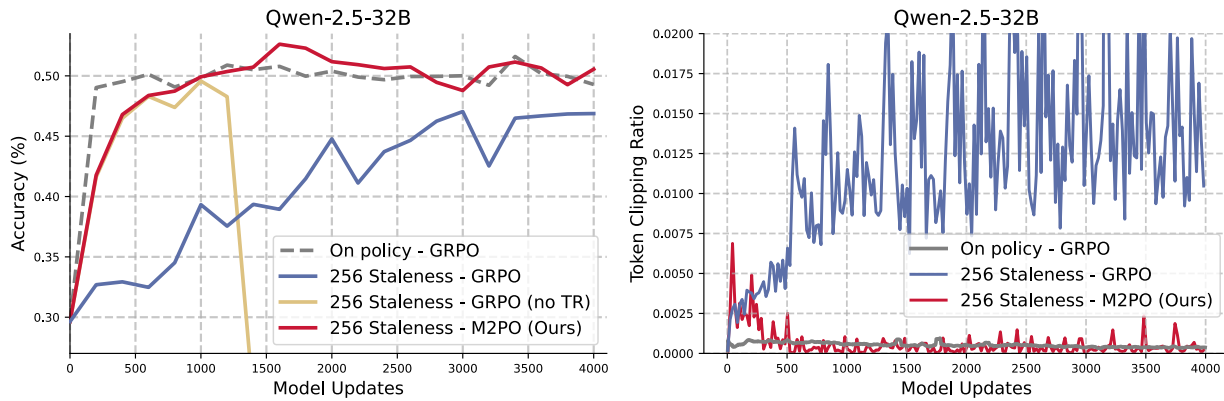


Figure 1 Comparison of on-policy GRPO and off-policy training under a staleness of 256 model updates on Qwen-2.5-32B. **Left:** Standard GRPO suffers from degradation with stale rollouts, while removing the trust region (GRPO no TR) reveals a clear *prosperity-before-collapse* phenomenon. In contrast, M2PO achieves stable training and matches on-policy performance even under high staleness. **Right:** Token clipping ratio comparison shows that M2PO dramatically reduces clipping events compared to GRPO with the same staleness, while avoiding training collapse.

1 Introduction

Reinforcement learning (RL) has been central to recent advances in large language model (LLM) reasoning, driving breakthroughs in systems like OpenAI’s o1 (OpenAI et al., 2024) and DeepSeek’s R1 (DeepSeek-AI et al., 2025; Team et al., 2025). Most existing RL algorithms (Schulman et al., 2017; Zheng et al., 2025b; Yu et al., 2025) for LLMs adopt an on-policy design, as it provides stable training and reliable performance, but the

strict requirement for fresh (or limited-staleness) rollouts at every update leads to substantial inefficiency and limits scalability. To overcome this bottleneck, a growing line of RL systems (Fu et al., 2025; Zhu et al., 2025; Noukhovitch et al., 2024; Zhong et al., 2025; He et al., 2025) have explored asynchronous designs that decouple rollout from training. Such approaches improve resource utilization and enable training to scale more efficiently across large and heterogeneous clusters, but their effectiveness fundamentally relies on the ability of RL algorithms to tolerate rollout staleness without sacrificing stability or performance.

However, under large rollout staleness, existing RL algorithms struggle to strike the right balance. Some methods (Schulman et al., 2017; Shao et al., 2024; Zheng et al., 2025a) can maintain stability, but they often suffer from noticeable performance degradation. Conversely, approaches designed to maximize performance (Fu et al., 2025; Chen et al., 2025; Su et al., 2025) tend to compromise stability, frequently leading to training collapse. On-policy methods provide both stability and strong performance, but their reliance on fresh or only slightly stale rollouts at every update imposes rigid constraints that hinder scalability. Consequently, an ideal off-policy RL algorithm for LLMs should enable effective reuse of trajectories collected under outdated policies to preserve strong performance under significant staleness, and ensure stable training that converges competitively with on-policy methods. Meeting these requirements is key to realizing off-policy RL as a truly scalable solution for aligning and fine-tuning large language models.

In this paper, we aim to investigate the underlying reasons for the limitations of off-policy RL in LLMs and to design an effective algorithm that fully leverages stale data to unlock its potential. We begin by revealing an intriguing *Prosperity before Collapse* phenomenon (Yellow curve in Figure 1 (left)): although RL training without a trust region eventually collapses on stale data, it initially achieves substantially higher performance than vanilla GRPO with ϵ -clipping. In some cases, it even matches the performance of the on-policy baseline. From this, we draw an important observation: *stale data can be as informative as data collected on-policy in RL for LLMs*, but the key challenge lies in how existing algorithms exploit it. In particular, vanilla GRPO performs poorly under staleness because stale-data training exhibits a substantially higher clipping rate, with many of the clipped updates occurring on informative high-entropy tokens (see Figure 4). This disproportionate clipping on crucial tokens hinders the full utilization of stale training data.

This pivotal token masking observation reveals that these high-entropy tokens play a dual role: they provide the most informative training signal but also introduce the greatest instability under staleness. Therefore, the key challenge is to retain as much learning signal from these tokens as possible without risking training collapse. Motivated by this, we propose **M2PO** (Second-Moment Trust Policy Optimization), a novel off-policy RL algorithm that constrains the second moment of importance weights. Unlike standard ϵ -clipping, which disproportionately suppresses high-entropy tokens and discards valuable learning signals, M2PO leverages the second-moment metric M_2 . This metric is both variance-sensitive, capturing instability introduced by high-entropy tokens, and statistically stable, avoiding the cancellation issues inherent to KL-based measures. By regularizing training at the batch level through M_2 , M2PO masks only extreme outliers while preserving the majority of informative updates. As a result, M2PO enables stable off-policy reinforcement learning with stale data, matching on-policy performance even under large staleness.

As illustrated in Figure 1 (left), even when trained exclusively on data stale by at least 256 model updates, M2PO achieves accuracy comparable to the on-policy baseline (red curve), demonstrating its ability to fully exploit stale data without sacrificing stability. M2PO achieves this through a more accurate and adaptive clipping strategy that clips substantially fewer tokens while maintaining training stability. As shown in Figure 1 (right), M2PO dramatically reduces the fraction of clipped tokens under high staleness (from 1.22% to 0.06% over the entire training process, see Figure 7b), thereby preserving more useful training information in stale data. To further validate M2PO effectiveness, we conduct an extensive evaluation of M2PO across six model scales (ranging from 1.7B to 32B) and eight math reasoning benchmarks in Section 6. The results show that M2PO consistently delivers strong performance across all training settings. M2PO also shows insensitivity to the choice of threshold, with a single value across all experiments, demonstrating its practicality and robustness.

2 Related Work

RLVR. Recent advances (DeepSeek-AI et al., 2025; Yu et al., 2025; Team et al., 2025; Gao et al., 2024) in LLM reasoning show that Reinforcement Learning with Verifiable Reward (RLVR), which relies on verifiable reward signals instead of model-generated scores, can effectively improve model reasoning ability. These gains are achieved using various policy optimization methods such as PPO (Ouyang et al., 2022) and GRPO (Shao

et al., 2024). Encouraged by the success of RLVR, a growing body of work (Kazemnejad et al., 2024; Yuan et al., 2025b,a; Yu et al., 2025; Liu et al., 2025; Luo et al., 2025a; Zhang et al., 2025; Hu, 2025; Xiong et al., 2025) has emerged to further improve reinforcement learning methods for LLM reasoning. For instance, methods such as VinePPO (Kazemnejad et al., 2024), VC-PPO (Yuan et al., 2025b), and VAPO (Yuan et al., 2025a) aim to enhance LLM reasoning by optimizing the value function.

Trust Region in RLVR. While RLVR has been widely adopted for fine-tuning LLMs, a key challenge lies in how to effectively constrain the trust region, not only to stabilize training but also to achieve better learning efficiency and overall performance. To address this, a growing line of work has proposed various strategies to control the policy update, ranging from ratio clipping (Yu et al., 2025), approximate trust region (Fu et al., 2025), sequence-level clipping (Zheng et al., 2025a), asymmetric trust region (Roux et al., 2025; Arnal et al., 2025), and gradient-preserving clipping (Su et al., 2025; Chen et al., 2025). For instance, AREAL (Fu et al., 2025) uses a more recent approximate policy to decide the trust region rather than the behavior model. GSPO (Zheng et al., 2025a) moves from token-level to sequence-level clipping by defining importance ratios on sequence likelihood. While these methods improve RLVR under moderate settings, most of them focus on relatively limited intra-iteration staleness (e.g., 8 or 16) and have not been thoroughly studied under larger off-policy gaps, like extreme staleness. In this work, our goal is to better understand the role of staleness in RLVR and to seek more effective ways of constraining the trust region in RLVR.

3 Background

3.1 Group Relative Policy Optimization (GRPO)

Group Relative Policy Optimization (GRPO) (Shao et al., 2024) is a variant of Proximal Policy Optimization (PPO) (Ouyang et al., 2022) tailored for language model fine-tuning. Instead of computing advantages using a value function, GRPO normalizes reward scores within groups of responses sampled for the same prompt, which largely improves the training efficiency, and aims to maximize the following objective:

$$\begin{aligned} \mathcal{J}_{GRPO}(\theta) = & \mathbb{E}[q \sim P(Q), \{o_i\}_{i=1}^G \sim \pi_{\theta_{old}}(O|q)] \\ & \frac{1}{G} \sum_{i=1}^G \left(\min \left(\frac{\pi_{\theta}(o_i|q)}{\pi_{\theta_{behav}}(o_i|q)} A_i, \text{clip} \left(\frac{\pi_{\theta}(o_i|q)}{\pi_{\theta_{behav}}(o_i|q)}, 1-\epsilon, 1+\epsilon \right) A_i \right) \right), \end{aligned} \quad (1)$$

where A_i is the advantage, computed using a group of rewards corresponding to the outputs within each group:

$$A_{i,t} = \frac{r_i - \text{mean}(\{R_i\}_{i=1}^G)}{\text{std}(\{R_i\}_{i=1}^G)}. \quad (2)$$

Similar to PPO, GRPO employs a clipping mechanism to stabilize updates. The ratio $r_i = \frac{\pi_{\theta}(o_i|q)}{\pi_{\theta_{old}}(o_i|q)}$ is clipped to $[1-\epsilon, 1+\epsilon]$, so that when $A_i > 0$ the policy cannot increase probability mass excessively, and when $A_i < 0$ it cannot over-penalize. This prevents large, unstable updates while still allowing normalized group advantages to guide learning.

3.2 Performance Degradation from Training with Stale Data

Stale- k RL training. To investigate the impact of stale data on reinforcement learning for large language models, we introduce Stale- k RL training, where the model is trained using data generated k model updates earlier in each training iteration. More specifically, in our training setup, each training step consists of four model updates, a configuration commonly used in recent work (Zheng et al., 2025b; Wang et al., 2025b; Yu et al., 2025; Chen et al., 2025; Zheng et al., 2025a). Thus, even stale-0 ($s=0$) training has a staleness between 0 and 3. stale-256 ($s=256$) training has a staleness between 256 and 259. During the first k model updates, since no stale model is yet available, the model is trained on data generated by the original base model, with different training data used in each iteration. In this setup, all training data after the initial phase comes from stale models,

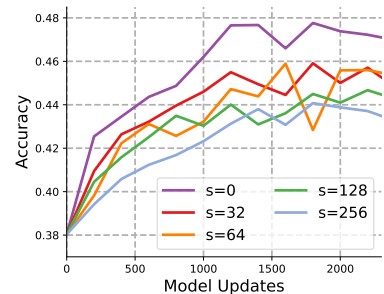


Figure 2 Average accuracy for RL with stale data on Qwen2.5-Math-7B.

allowing us to study how stale data affects the dynamics and effectiveness of RL training. More training details can be found at Appendix B.

As shown in Figure 2, we train Qwen2.5-Math-7B (Yang et al., 2024) with GRPO under varying staleness levels and report test accuracy. The results reveal a clear trend: as staleness increases, model performance degrades and convergence slows. In particular, low-staleness training achieves higher accuracy, whereas high-staleness training converges more slowly to lower performance.

4 Prosperity before Collapse: Stale Data Contain Enough Training Information in RL on LLMs

In this section, we investigate why RL on LLM deteriorates when trained on stale data generated by earlier policies. First, we reveal an intriguing *prosperity-before-collapse* phenomenon: although off-policy RL training without a trust region eventually collapses on stale data, it achieves substantially higher performance than GRPO with ϵ -clipping before collapse, even matching on-policy results. Next, we study the causes of GRPO’s inferior performance when trained with stale data.

Prosperity before collapse: training without a trust region. To disentangle whether the performance drop stems from stale data generated by highly shifted old policies or from biases introduced by the training algorithm, we remove the trust region entirely to remove bias from the training algorithm. Surprisingly, we observe a distinct *prosperity-before-collapse* phenomenon. As shown in Figure 1 and Figure 3, although training without a trust region eventually collapses, it achieves substantially better performance prior to collapse. In fact, under stale data ($s=256$), the no-clipping setting outperforms clipped training, sometimes even matching on-policy baselines.

Pivotal token masking by ϵ -clipping when training with stale data. As also discussed in recent work (Su et al., 2025; Chen et al., 2025), ϵ -clipping may inadvertently mask important tokens, preventing them from contributing useful training signals. We extend this observation to the asynchronous setting and show that the problem becomes substantially more severe when training with stale data, since larger staleness induces a greater mismatch between the behavior and target policies. As illustrated in Figure 4a, the clipping ratio increases sharply under large staleness ($s=256$), while remaining much lower in the on-policy baseline.

To better understand this phenomenon, we conduct a quantitative analysis on 90 million training tokens collected during Qwen2.5-Math-7B training with staleness 256. Specifically, we gather all training tokens generated between 800 and 1200 model updates, ensuring the model is already in a stable training phase but before convergence. Figure 4b shows a clear trend: as $|r-1|$ increases, the average token entropy also rises. This indicates that ϵ -clipping disproportionately prunes high-entropy tokens, which are typically the most informative for model improvement. Consequently, clipping under stale data leads to degraded performance.

This observation reveals a dilemma: while high-entropy tokens are crucial for learning progress,

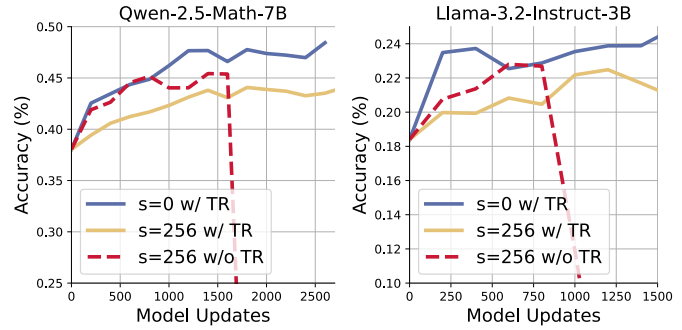


Figure 3 Prosperity before Collapse. Training without a trust region ($\epsilon = \infty$) under stale data ($s=256$) initially achieves higher performance than clipped training, sometimes even matching the on-policy baseline ($s=0$). However, it eventually collapses due to uncontrolled variance.

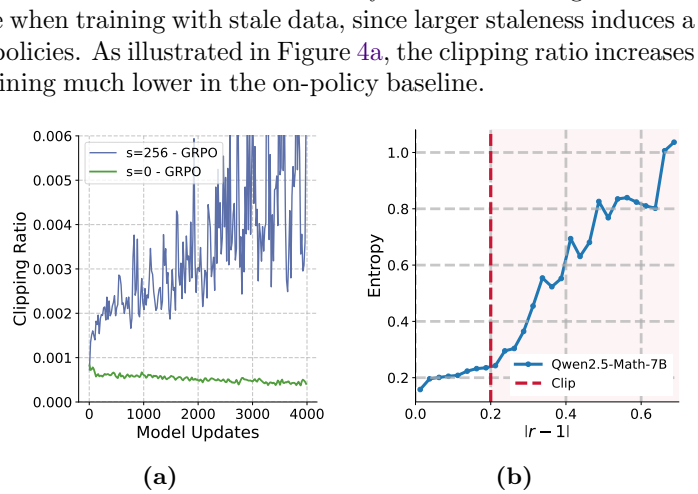


Figure 4 (a) Clipping ratio during training on the Qwen-2.5-Math-7B model. (b) Relationship between average token entropy and the distance between the importance sampling ratio and 1.

they also introduce instability in the off-policy setting, which motivates our key research question:

Can a more accurate and adaptive trust region strategy preserve the benefits of stale data while ensuring stable training?

5 Second-Moment Trust Policy Optimization

In this section, we propose Second-Moment Trust Policy Optimization (M2PO), a novel policy optimization algorithm providing a more effective trust region for off-policy training with stale data. As discussed in Section 4, as high-entropy tokens are a double-edged sword, the key challenge in designing an effective trust region algorithm is how to best harness the rich information in high-entropy tokens without letting them destabilize training.

5.1 Measuring Distribution Gap with the Second Moment

The main source of instability in off-policy RL lies in the distributional mismatch between the behavior policy that generates training data and the current policy being optimized (Schulman et al., 2015, 2017). As the divergence between these two distributions grows, importance sampling corrections produce high-variance gradient estimates, leading to noisy and unreliable updates. Our motivation is therefore to constrain the distributional gap between π_{behav} and π_θ at the batch level, directly coupling the constraint with model updates while preventing over-constraining of token-level variations.

A natural choice to measure distribution is the batch-level KL divergence, a metric widely adopted to monitor stability in RL:

$$\hat{KL} = \frac{1}{N} \sum_{i=1}^N \hat{KL}_i = -\frac{1}{N} \sum_{i=1}^N \log r_i = -\frac{1}{N} \sum_{i=1}^N \log \frac{\pi_\theta(a_i | s_i)}{\pi_{\text{behav}}(a_i | s_i)}, \quad (3)$$

where N is the number of tokens in a batch.

However, batch-level KL suffers from two key limitations. First, because it is computed from single-sample estimates, individual \hat{KL}_i can be positive or negative, leading to *cancellation effects* where large deviations offset each other and produce deceptively small KL values. Second, tokens with large ratios ($r_i > 1$) are not properly constrained, as their negative \hat{KL}_i actually decreases the estimated KL, even though such tokens can contribute to training instability (Schulman et al., 2017).

To overcome these limitations, we propose to use the second moment of the log-ratio to measure the distribution gap between behavior and current policy. Formally, we define

$$\hat{M}_2 = \frac{1}{N} \sum_{i=1}^N \hat{M}_{2,i} = \frac{1}{N} \sum_{i=1}^N (\log r_i)^2 = \frac{1}{N} \sum_{i=1}^N [\log \frac{\pi_\theta(a_i | s_i)}{\pi_{\text{behav}}(a_i | s_i)}]^2, \quad (4)$$

This choice is motivated by two key advantages of \hat{M}_2 over the batch \hat{KL} . First, each per-token estimate $\hat{M}_{2,i} = (\log r_i)^2$ is always non-negative, so the constraint can be reliably applied even when $r > 1$. Second, while the batch KL only measures the mean shift between policies, M_2 also reflects the variance of importance weights. This makes \hat{M}_2 more sensitive to outliers and noisy tokens with extreme ratios r_i ¹.

Furthermore, Theorem 5.1 shows that although M_2 does not directly constrain $r - 1$ like ϵ clipping, it nevertheless provides an upper bound on the Pearson chi-square divergence $\mathbb{E}[(r - 1)^2]$ between the new and behavior policies. The proof is provided in Appendix C.

¹A potential alternative is to use $\sum_{i=1}^N |\hat{KL}_i|/N$. While this absolute KL estimate can also work empirically, it is less sensitive to variance compared to M_2 . Moreover, M2 provides an upper bound for this absolute KL estimate, as $E[|r|] \leq \sqrt{E[r^2]}$. Therefore, we adopt M_2 in our method.

Theorem 5.1 (Bounding χ^2 by M_2). Let $r = \frac{\pi_{\text{new}}}{\pi_{\text{behav}}}$ be the importance ratio and assume $1/R \leq r \leq R$. Define the log-ratio second moment

$$M_2 = \mathbb{E}_{a \sim \pi_{\text{behav}}} [(\log(r(a))^2].$$

Let the Pearson chi-square divergence between π_{new} and π_{behav} be

$$\chi^2(\pi_{\text{new}} \parallel \pi_{\text{behav}}) = \mathbb{E}_{a \sim \pi_{\text{behav}}} \left[\left(\frac{\pi_{\text{new}}(a)}{\pi_{\text{behav}}(a)} - 1 \right)^2 \right] = \mathbb{E}_{\pi_{\text{behav}}} [(r-1)^2].$$

Then

$$\chi^2(\pi_{\text{new}} \parallel \pi_{\text{behav}}) \leq R^2 M_2.$$

5.2 Second-Moment Trust Policy Optimization

As illustrated in Algorithm 1, to maintain training stability, M2PO applies a masking strategy that selectively excludes tokens until the batch-level \hat{M}_2 of the remaining tokens falls below a predefined threshold τ_{M_2} . Importantly, we observe that τ_{M_2} is not a sensitive hyperparameter (see Figure 8). Across all our experiments, we consistently set $\tau_{M_2} = 0.04$, and this single setting proved effective for stabilizing training in all training scenarios.

Only constrain trust-region tokens. Although the PPO loss clips the ratio on both the upper and lower sides, due to the use of the `min` operator, not all tokens are actually clipped. In practice, clipping only occurs for tokens where $A > 0$ and $r > 1$, or $A < 0$ and $r < 1$. Following the PPO setting, we therefore apply the M_2 constraint exclusively to tokens that satisfy these conditions. Finally, with the result mask \mathbf{M} , we update the policy by maximizing the following objective²:

$$\mathcal{J}_{\text{M2PO}}(\theta) = \frac{1}{\sum_{i=1}^G |o_i|} \sum_{i=1}^G \sum_{t=1}^{|o_i|} \mathbf{M}_{i,t} \frac{\pi_\theta(o_i|q)}{\pi_{\theta_{\text{behav}}}(o_i|q)} A_{i,t}, \quad \mathbf{M}_{i,t} \in \{0,1\}, \quad (5)$$

where A_i denotes the advantage, computed using the grouped advantage in Equation 2.

6 Experiments

In this section, we present an extensive evaluation across six models (from 1.7B to 32B) on eight benchmarks. The results demonstrate that, even when trained with extremely stale data, M2PO achieves performance comparable to on-policy GRPO and significantly outperforms other baselines:

- In Section 6.2, we show that M2PO achieves **accuracy on par with on-policy baselines** under large staleness ($s=256$), and outperforms baselines by up to 11.2% in average accuracy.
- In Section 6.3, we provide a detailed analysis of how M2PO boosts off-policy RL performance while preserving training stability. We also show that its sole threshold hyperparameter τ_{M_2} is insensitive to variation, ensuring ease of use in practice.

6.1 Experimental Settings

Models & Datasets. To verify the effectiveness of our method, we extensively evaluate M2PO on six models: Qwen2.5-Math-7B (Yang et al., 2024), Llama-3.2-3B-Instruct (Dubey et al., 2024), Qwen3-Base-1.7B/4B/8B (Yang et al., 2025), and Qwen2.5-32B (Yang et al., 2024). For Qwen2.5-Math-7B, we use a context length of 4k, which is the maximum for this series, while for all other models the context length is set to 16k. For training, we adopt the DeepScaleR (Luo et al., 2025b) math dataset.

²In our loss, we average over all tokens rather than only the unmasked ones. This choice is intended to better mimic the behavior of PPO-style clipping. However, since the masking ratio is typically very small (see Section 6.3), the difference between the two averaging strategies is negligible in practice.

Table 1 Performance (%) comparison across eight math reasoning benchmarks using models from 1.7B to 32B parameters. We report results for GRPO, GSPO, and M2PO under both on-policy ($s=0$) and off-policy ($s=256$) settings. Underlined numbers denote the best average accuracy, while **bold** numbers highlight the best average accuracy under stale rollouts ($s=256$). M2PO consistently improves stability under staleness and achieves higher average accuracy than GRPO.

| Method | S | AIME24/25 | AMC23/24 | Math500 | Gaokao | Miner. | Olymp. | Avg. |
|------------------------------|-----|-------------|-------------|---------|--------|--------|--------|-------------|
| <i>Llama-3.2-3B-Instruct</i> | | | | | | | | |
| GRPO | 0 | 11.0 / 2.3 | 31.3 / 17.2 | 53.6 | 42.99 | 23.1 | 20.3 | 25.2 |
| GRPO | 256 | 9.6 / 0.4 | 25.0 / 13.9 | 52.4 | 42.08 | 17.6 | 18.8 | 22.5 |
| GSPO | 256 | 9.0 / 0.2 | 30.0 / 14.4 | 50.6 | 40.65 | 18.8 | 17.3 | 22.6 |
| M2PO (Ours) | 256 | 10.4 / 4.4 | 33.8 / 17.8 | 52.0 | 44.48 | 21.2 | 18.1 | 25.3 |
| <i>Qwen2.5-Math-7B</i> | | | | | | | | |
| GRPO | 0 | 39.6 / 17.5 | 63.8 / 46.7 | 82.3 | 64.1 | 36.7 | 43.6 | <u>49.3</u> |
| GRPO | 256 | 29.4 / 12.9 | 64.4 / 39.4 | 80.5 | 63.2 | 33.1 | 43.1 | 45.7 |
| GSPO | 256 | 27.3 / 13.1 | 63.8 / 36.7 | 79.0 | 62.2 | 33.5 | 41.9 | 44.7 |
| M2PO (Ours) | 256 | 33.3 / 17.5 | 63.8 / 40.6 | 84.0 | 66.4 | 38.1 | 47.1 | 48.8 |
| <i>Qwen3-Base-1.7B</i> | | | | | | | | |
| GRPO | 0 | 7.5 / 7.5 | 40.6 / 26.1 | 67.2 | 55.9 | 28.9 | 30.5 | 33.0 |
| GRPO | 256 | 8.5 / 4.8 | 34.4 / 25.0 | 64.3 | 52.7 | 26.0 | 27.6 | 30.4 |
| GSPO | 256 | 6.9 / 4.0 | 39.4 / 18.9 | 65.0 | 53.1 | 26.5 | 27.5 | 30.1 |
| M2PO (Ours) | 256 | 14.0 / 6.5 | 48.1 / 27.8 | 71.8 | 59.5 | 29.4 | 35.6 | 36.6 |
| <i>Qwen3-Base-4B</i> | | | | | | | | |
| GRPO | 0 | 22.9 / 20.2 | 63.8 / 53.9 | 84.6 | 69.8 | 40.2 | 50.5 | 50.7 |
| GRPO | 256 | 14.0 / 9.6 | 51.9 / 32.8 | 76.8 | 61.7 | 34.4 | 39.8 | 40.1 |
| GSPO | 256 | 17.9 / 15.4 | 55.6 / 38.3 | 76.8 | 62.3 | 35.1 | 44.3 | 43.2 |
| M2PO (Ours) | 256 | 26.7 / 21.0 | 64.4 / 49.4 | 85.8 | 70.3 | 40.5 | 52.3 | 51.3 |
| <i>Qwen3-Base-8B</i> | | | | | | | | |
| GRPO | 0 | 26.7 / 19.4 | 76.9 / 52.8 | 87.7 | 71.6 | 41.2 | 52.8 | 53.6 |
| GRPO | 256 | 21.0 / 13.1 | 63.8 / 40.0 | 81.8 | 67.8 | 38.5 | 47.4 | 46.7 |
| M2PO (Ours) | 256 | 30.2 / 23.1 | 71.3 / 56.7 | 87.2 | 75.1 | 42.6 | 54.8 | 55.1 |
| <i>Qwen2.5-32B</i> | | | | | | | | |
| GRPO | 0 | 24.4 / 18.3 | 71.9 / 46.7 | 85.4 | 71.9 | 41.4 | 52.9 | 51.6 |
| GRPO | 256 | 20.4 / 9.6 | 68.1 / 41.1 | 83.0 | 67.3 | 40.9 | 45.9 | 47.0 |
| M2PO (Ours) | 256 | 24.8 / 19.4 | 76.3 / 50.0 | 85.7 | 71.7 | 41.5 | 51.7 | 52.6 |

Training & Evaluation. Our method is implemented based on verl (Sheng et al., 2024) pipeline and uses vLLM (Kwon et al., 2023) for rollout. We use a mix of H100 and H200 servers for training, depending on resource availability. For benchmark datasets, we use eight widely used complex mathematical reasoning benchmarks to evaluate the performance of trained models: Math500 (Hendrycks et al., 2021; Lightman et al., 2023), AIME24/25 (Art of Problem Solving, 2024a), AMC23/24 (Art of Problem Solving, 2024b), Minerva Math (Lewkowycz et al., 2022), Gaokao (Zhang et al., 2023), Olympiad Bench (He et al., 2024). Similar to (Wang et al., 2025b; Zheng et al., 2025b), we evaluate models on those benchmarks every 50 steps and report the performance of the checkpoint that obtains the best average performance on eight benchmarks. For GRPO, we adopt the commonly used clipping parameter $\epsilon=0.2$, while for the other baselines, we follow the recommended values reported in their respective papers. We include more detailed experimental settings in Appendix B.

6.2 Performance Comparison on Training with Staleness

Prosperity without collapse: Stable off-policy training without performance degradation using M2PO. To verify the effectiveness of M2PO, Table 1 presents a comprehensive comparison of math reasoning performance across eight benchmarks using models from four different families and scales, ranging from 1.7B to 32B parameters. We evaluate multiple reinforcement learning methods under both on-policy and off-policy settings, including GRPO, GSPO, and our proposed M2PO. The results show that while

both GRPO and GSPO often suffer significant performance drops under large staleness, M2PO consistently achieves comparable accuracy to the on-policy baseline in all training settings. Surprisingly, we notice that, in some model settings, M2PO with $s = 256$ even achieves a better performance than M2PO with $s = 0$. For instance, on the Qwen3-Base-1.7B model, we observe that M2PO with $s = 256$ (36.6%) outperforms GRPO with $s = 0$ (33.0%). A potential explanation is that small effective staleness (e.g., $s = 0$ corresponding to delays between 0 and 3) can still adversely affect training stability. Our further analysis in Figure 7 supports this view, showing that M2PO with $s = 256$ exhibits an even lower clipping ratio than GRPO with $s = 0$. Overall, these results show that M2PO remains robust and effective, sustaining stable, high performance even under extreme off-policy conditions.

In addition to the final accuracy comparison in Table 1, we also analyze the training dynamics of accuracy and reward of Qwen-2.5-32B models. As shown in Figure 1, M2PO with $s = 256$ initially falls behind the on-policy baseline but quickly catches up, eventually matching its performance, while converging much faster and achieving higher accuracy than GRPO under the same staleness. This highlights that M2PO not only maintains comparable final accuracy but also accelerates convergence when training with stale data. Figure 5 shows a similar trend in the reward curves. M2PO with $s = 256$ also starts off behind the on-policy baseline due to the initial plateau caused by using data generated from the base model, but it quickly catches up and aligns closely with the $s = 0$ trajectory. In contrast, GRPO with $s = 256$ consistently underperforms across the entire training trajectory.

Performance of other baselines under staleness. A number of prior works have proposed alternative trust region strategies beyond ϵ -clipping, including GSPO (Zheng et al., 2025a), AREAL (Fu et al., 2025), TOPR (Roux et al., 2025), GPPO (Su et al., 2025), and CISPO (Chen et al., 2025). *Despite not being designed to handle the extreme staleness studied in this paper*, we also evaluate these methods under our setting with $s = 256$ for completeness and comparison. Among these methods, GSPO is the only one that preserves training stability, though it still exhibits a noticeable performance drop under high staleness (see Table 1). For the other methods, as shown in Figure 6, most encounter substantial difficulties in maintaining training stability and tend to break down early in training. These observations suggest that while existing approaches can be effective under moderately stale settings, they face significant challenges when extended to larger staleness, highlighting the need for a more robust and effective solution.

6.3 Analysis and Ablation Study

Stable training with reduced clipping. Figure 7(a)(b) illustrates the clipping dynamics of GRPO and our proposed M2PO under different staleness settings. In Figure 7a, we report results on Qwen-3-Base-1.7B. Under large staleness ($s = 256$), GRPO exhibits frequent clipping events, with the ratio increasing sharply and remaining high during most of the training. In contrast, M2PO under the same staleness maintains an exceptionally low clipping ratio, comparable to or even lower than the on-policy GRPO baseline ($s = 0$). Notably, M2PO with

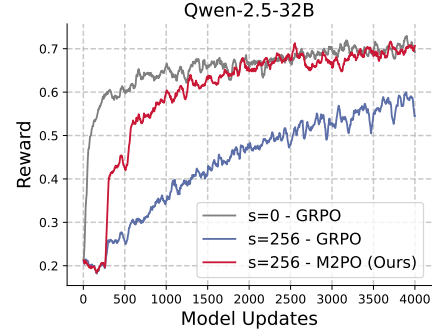


Figure 5 Training reward on Qwen-2.5-32B.

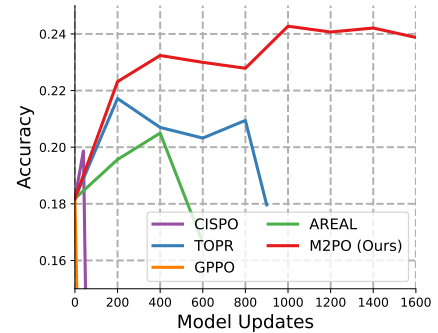


Figure 6 Methods comparison under staleness ($s = 256$) on Llama-Instruct-3B.

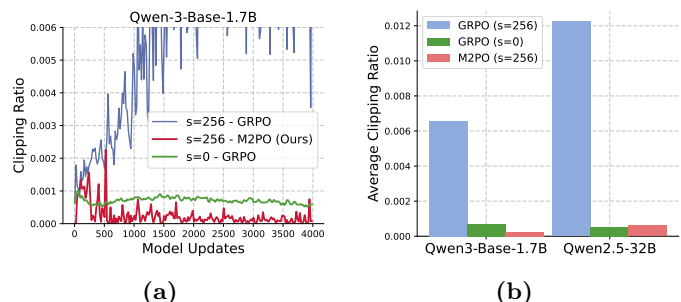


Figure 7 (a) Clipping ratio dynamics during RL on the Qwen-3-Base-1.7B model. (b) Comparison of the average clipping ratio across models and methods.

$s=256$ exhibits less clipping than GRPO with $s=0$, which explains why M2PO with $s=256$ achieves higher accuracy than GRPO with $s=0$ in Table 1. Figure 1 shows the same comparison on Qwen-2.5-32B. A similar trend holds: GRPO with $s=256$ suffers from substantial clipping, whereas M2PO effectively suppresses unnecessary clipping, remaining close to the on-policy baseline.

Figure 7b summarizes the average clipping ratio across the entire training process. On Qwen-3-Base-1.7B, GRPO with $s=256$ reaches an average clipping ratio of 0.66%, compared to 0.07% for GRPO with $s=0$ and only 0.02% for M2PO with $s=256$. On Qwen-2.5-32B, GRPO with $s=256$ averages 1.22%, while GRPO with $s=0$ records 0.05% and M2PO with $s=256$ maintains a similarly low ratio of 0.06%. These results show that M2PO reduces clipping by over an order of magnitude compared to GRPO, thereby enabling stable and efficient training by clipping only when necessary.

Robustness to the choice of τ_{M_2} . Figure 8 shows that performance is not highly sensitive to the choice of τ_{M_2} . Accuracy remains stable across a broad range, only dropping when τ_{M_2} is set extremely small (overly restrictive constraint) or very large (training collapse). This explains why a single setting of $\tau_{M_2}=0.04$ works robustly across all training settings in our paper.

Training dynamics on KL and M_2 . Figure 9 shows the impact of M2PO masking on training stability. Figure 9a shows that the average M_2 without masking exhibits frequent spikes throughout training, indicating instability in the second-moment estimates (blue curve). Applying M2PO masking effectively suppresses these fluctuations and maintains consistently low M_2 values, leading to more stable updates (red curve). Figure 9b compares the KL divergence across different methods. Although M2PO with $s=256$ involves substantially less clipping than GRPO (shown in Figure 7), it maintains a more stable divergence than GRPO with $s=256$. These results indicate that M2PO performs clipping in a more precise and adaptive manner, ensuring training stability with substantially less reliance on clipping. These results demonstrate that M2PO enables more precise and adaptive clipping, achieving training stability while relying on significantly fewer clipping operations, and thereby attaining better performance without risking training collapse.

7 Conclusion

In this work, we investigated why off-policy RL for LLMs often fails under stale data and uncovered the *prosperity-before-collapse* phenomenon: training without a trust region initially outperforms standard methods, showing that stale data can be as informative as on-policy trajectories, but eventually collapses due to instability. Motivated by this observation, we proposed **M2PO**, which constrains the second moment of importance weights to provide a variance-sensitive and stable trust region. This design suppresses extreme outliers while preserving informative high-entropy tokens, enabling stable training that matches on-policy performance even under extreme staleness. Extensive experiments further demonstrate that M2PO significantly reduces clipping and is highly insensitive to its threshold, highlighting its practicality and scalability for efficient RL with LLMs.

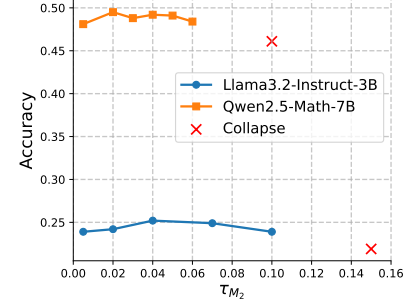


Figure 8 Ablation study of the τ_{M_2} threshold on Llama-3.2-3B-Instruct and Qwen2.5-Math-7B.

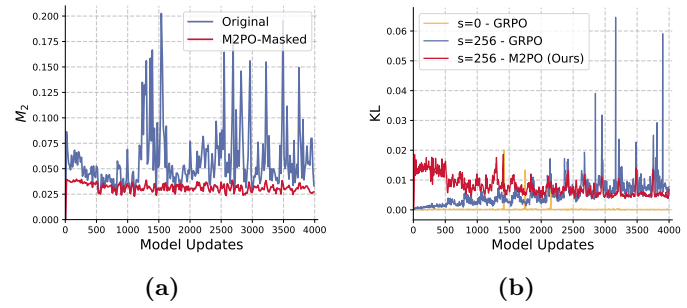


Figure 9 (a) Average M_2 in each model updates with and without M2PO masking on Qwen-2.5-32B, showing that masking effectively suppresses spikes and stabilizes the M_2 throughout training. (b) Average KL divergence in each model updates on Qwen-2.5-32B under different methods.

These results demonstrate that M2PO enables more precise and adaptive clipping, achieving training stability while relying on significantly fewer clipping operations, and thereby attaining better performance without risking training collapse.

References

Charles Arnal, GaĂĂTtan Narozniak, Vivien Cabannes, Yunhao Tang, Julia Kempe, and Remi Munos. Asymmetric reinforce for off-policy reinforcement learning: Balancing positive and negative rewards. *arXiv preprint arXiv:2506.20520*, 2025.

Art of Problem Solving. Aime problems and solutions. https://artofproblemsolving.com/wiki/index.php/AIME_Problems_and_Solutions, 2024a. Accessed: 2025-04-20.

Art of Problem Solving. Amc problems and solutions. https://artofproblemsolving.com/wiki/index.php?title=AMC_Problems_and_Solutions, 2024b. Accessed: 2025-04-20.

Aili Chen, Aonian Li, Bangwei Gong, Binyang Jiang, Bo Fei, Bo Yang, Boji Shan, Changqing Yu, Chao Wang, Cheng Zhu, et al. Minimax-m1: Scaling test-time compute efficiently with lightning attention. *arXiv preprint arXiv:2506.13585*, 2025.

DeepSeek-AI, Daya Guo, Dejian Yang, Haowei Zhang, Junxiao Song, Ruoyu Zhang, Runxin Xu, Qihao Zhu, Shirong Ma, Peiyi Wang, Xiao Bi, Xiaokang Zhang, Xingkai Yu, Yu Wu, Z. F. Wu, Zhibin Gou, Zhihong Shao, Zhuoshu Li, Ziyi Gao, Aixin Liu, Bing Xue, Bingxuan Wang, Bochao Wu, Bei Feng, Chengda Lu, Chenggang Zhao, Chengqi Deng, Chenyu Zhang, Chong Ruan, Damai Dai, Deli Chen, Dongjie Ji, Erhang Li, Fangyun Lin, Fucong Dai, Fuli Luo, Guangbo Hao, Guanting Chen, Guowei Li, H. Zhang, Han Bao, Hanwei Xu, Haocheng Wang, Honghui Ding, Huajian Xin, Huazuo Gao, Hui Qu, Hui Li, Jianzhong Guo, Jiashi Li, Jiawei Wang, Jingchang Chen, Jingyang Yuan, Junjie Qiu, Junlong Li, J. L. Cai, Jiaqi Ni, Jian Liang, Jin Chen, Kai Dong, Kai Hu, Kaige Gao, Kang Guan, Kexin Huang, Kuai Yu, Lean Wang, Lecong Zhang, Liang Zhao, Litong Wang, Liyue Zhang, Lei Xu, Leyi Xia, Mingchuan Zhang, Minghua Zhang, Minghui Tang, Meng Li, Miaojun Wang, Mingming Li, Ning Tian, Panpan Huang, Peng Zhang, Qiancheng Wang, Qinyu Chen, Qiushi Du, Ruiqi Ge, Ruisong Zhang, Ruizhe Pan, Runji Wang, R. J. Chen, R. L. Jin, Ruyi Chen, Shanghao Lu, Shangyan Zhou, Shanhua Chen, Shengfeng Ye, Shiyu Wang, Shuiping Yu, Shunfeng Zhou, Shuting Pan, S. S. Li, Shuang Zhou, Shaoqing Wu, Shengfeng Ye, Tao Yun, Tian Pei, Tianyu Sun, T. Wang, Wangding Zeng, Wanja Zhao, Wen Liu, Wenfeng Liang, Wenjun Gao, Wenqin Yu, Wentao Zhang, W. L. Xiao, Wei An, Xiaodong Liu, Xiaohan Wang, Xiaokang Chen, Xiaotao Nie, Xin Cheng, Xin Liu, Xin Xie, Xingchao Liu, Xinyu Yang, Xinyuan Li, Xuecheng Su, Xuheng Lin, X. Q. Li, Xiangyue Jin, Xiaojin Shen, Xiaosha Chen, Xiaowen Sun, Xiaoxiang Wang, Xinnan Song, Xinyi Zhou, Xianzu Wang, Xinxia Shan, Y. K. Li, Y. Q. Wang, Y. X. Wei, Yang Zhang, Yanhong Xu, Yao Li, Yao Zhao, Yaofeng Sun, Yaohui Wang, Yi Yu, Yichao Zhang, Yifan Shi, Yiliang Xiong, Ying He, Yishi Piao, Yisong Wang, Yixuan Tan, Yiyang Ma, Yiyuan Liu, Yongqiang Guo, Yuan Ou, Yuduan Wang, Yue Gong, Yuheng Zou, Yujia He, Yunfan Xiong, Yuxiang Luo, Yuxiang You, Yuxuan Liu, Yuyang Zhou, Y. X. Zhu, Yanhong Xu, Yanping Huang, Yaohui Li, Yi Zheng, Yuchen Zhu, Yunxian Ma, Ying Tang, Yukun Zha, Yuting Yan, Z. Z. Ren, Zehui Ren, Zhangli Sha, Zhe Fu, Zhean Xu, Zhenda Xie, Zhengyan Zhang, Zhewen Hao, Zhicheng Ma, Zhigang Yan, Zhiyu Wu, Zihui Gu, Zijia Zhu, Zijun Liu, Zilin Li, Ziwei Xie, Ziyang Song, Zizheng Pan, Zhen Huang, Zhipeng Xu, Zhongyu Zhang, and Zhen Zhang. Deepseek-r1: Incentivizing reasoning capability in llms via reinforcement learning. *arXiv preprint arXiv:2501.12948*, 2025.

Abhimanyu Dubey, Abhinav Jauhri, Abhinav Pandey, Abhishek Kadian, Ahmad Al-Dahle, Aiesha Letman, Akhil Mathur, Alan Schelten, Amy Yang, Angela Fan, et al. The llama 3 herd of models. *arXiv e-prints*, pages arXiv–2407, 2024.

Wei Fu, Jiaxuan Gao, Xujie Shen, Chen Zhu, Zhiyu Mei, Chuyi He, Shusheng Xu, Guo Wei, Jun Mei, Jiashu Wang, et al. Areal: A large-scale asynchronous reinforcement learning system for language reasoning. *arXiv preprint arXiv:2505.24298*, 2025.

Jiaxuan Gao, Shusheng Xu, Wenjie Ye, Weilin Liu, Chuyi He, Wei Fu, Zhiyu Mei, Guangju Wang, and Yi Wu. On designing effective rl reward at training time for llm reasoning. *arXiv preprint arXiv:2410.15115*, 2024.

Chaoqun He, Renjie Luo, Yuzhuo Bai, Shengding Hu, Zhen Leng Thai, Junhao Shen, Jinyi Hu, Xu Han, Yujie Huang, Yuxiang Zhang, et al. Olympiadbench: A challenging benchmark for promoting agi with olympiad-level bilingual multimodal scientific problems. *arXiv preprint arXiv:2402.14008*, 2024.

Jingkai He, Tianjian Li, Erhu Feng, Dong Du, Qian Liu, Tao Liu, Yubin Xia, and Haibo Chen. History rhymes: Accelerating llm reinforcement learning with rhymarl. *arXiv preprint arXiv:2508.18588*, 2025.

Dan Hendrycks, Collin Burns, Saurav Kadavath, Akul Arora, Steven Basart, Eric Tang, Dawn Song, and Jacob Steinhardt. Measuring mathematical problem solving with the math dataset. *NeurIPS*, 2021.

Jian Hu. Reinforce++: A simple and efficient approach for aligning large language models. *arXiv preprint arXiv:2501.03262*, 2025.

Amirhossein Kazemnejad, Milad Aghajohari, Eva Portelance, Alessandro Sordoni, Siva Reddy, Aaron Courville, and

Nicolas Le Roux. Vineppo: Unlocking rl potential for llm reasoning through refined credit assignment. *arXiv preprint arXiv:2410.01679*, 2024.

Woosuk Kwon, Zhuohan Li, Siyuan Zhuang, Ying Sheng, Lianmin Zheng, Cody Hao Yu, Joseph Gonzalez, Hao Zhang, and Ion Stoica. Efficient memory management for large language model serving with pagedattention. In *Proceedings of the 29th Symposium on Operating Systems Principles*, pages 611–626, 2023.

Aitor Lewkowycz, Anders Andreassen, David Dohan, Ethan Dyer, Henryk Michalewski, Vinay Ramasesh, Ambrose Slone, Cem Anil, Imanol Schlag, Theo Gutman-Solo, et al. Solving quantitative reasoning problems with language models. *Advances in Neural Information Processing Systems*, 35:3843–3857, 2022.

Hunter Lightman, Vineet Kosaraju, Yura Burda, Harri Edwards, Bowen Baker, Teddy Lee, Jan Leike, John Schulman, Ilya Sutskever, and Karl Cobbe. Let’s verify step by step. *arXiv preprint arXiv:2305.20050*, 2023.

Zichen Liu, Changyu Chen, Wenjun Li, Penghui Qi, Tianyu Pang, Chao Du, Wee Sun Lee, and Min Lin. Understanding r1-zero-like training: A critical perspective. *arXiv preprint arXiv:2503.20783*, 2025.

Ilya Loshchilov and Frank Hutter. Decoupled weight decay regularization. In *International Conference on Learning Representations*, 2019.

Michael Luo, Sijun Tan, Roy Huang, Xiaoxiang Shi, Rachel Xin, Colin Cai, Ameen Patel, Alpay Ariyak, Qingyang Wu, Ce Zhang, et al. Deepcoder: A fully open-source 14b coder at o3-mini level, 2025a.

Michael Luo, Sijun Tan, Justin Wong, Xiaoxiang Shi, William Tang, Manan Roongta, Colin Cai, Jeffrey Luo, Tianjun Zhang, Erran Li, Raluca Ada Popa, and Ion Stoica. Deepscaler: Surpassing o1-preview with a 1.5b model by scaling rl. <https://pretty-radio-b75.notion.site/DeepScaleR-Surpassing-O1-Preview-with-a-1-5B-Model-by-Scaling-RL-19681902c1468005bed8ca303013a4e2>, 2025b. Notion Blog.

Michael Noukhovitch, Shengyi Huang, Sophie Xhonneux, Arian Hosseini, Rishabh Agarwal, and Aaron Courville. Asynchronous rlhf: Faster and more efficient off-policy rl for language models. *arXiv preprint arXiv:2410.18252*, 2024.

OpenAI, :, Aaron Jaech, Adam Kalai, Adam Lerer, Adam Richardson, Ahmed El-Kishky, Aiden Low, Alec Helyar, Aleksander Madry, Alex Beutel, Alex Carney, Alex Iftimie, Alex Karpenko, Alex Tachard Passos, Alexander Neitz, Alexander Prokofiev, Alexander Wei, Allison Tam, Ally Bennett, Ananya Kumar, Andre Saraiva, Andrea Vallone, Andrew Duberstein, Andrew Kondrich, Andrey Mishchenko, Andy Applebaum, Angela Jiang, Ashvin Nair, Barret Zoph, Behrooz Ghorbani, Ben Rossen, Benjamin Sokolowsky, Boaz Barak, Bob McGrew, Borys Minaiev, Botaao Hao, Bowen Baker, Brandon Houghton, Brandon McKinzie, Brydon Eastman, Camillo Lugaressi, Cary Bassin, Cary Hudson, Chak Ming Li, Charles de Bourcy, Chelsea Voss, Chen Shen, Chong Zhang, Chris Koch, Chris Orsinger, Christopher Hesse, Claudia Fischer, Clive Chan, Dan Roberts, Daniel Kappler, Daniel Levy, Daniel Selsam, David Dohan, David Farhi, David Mely, David Robinson, Dimitris Tsipras, Doug Li, Dragos Oprica, Eben Freeman, Eddie Zhang, Edmund Wong, Elizabeth Proehl, Enoch Cheung, Eric Mitchell, Eric Wallace, Erik Ritter, Evan Mays, Fan Wang, Felipe Petroski Such, Filippo Raso, Florencia Leoni, Foivos Tsimpourlas, Francis Song, Fred von Lohmann, Freddie Sulit, Geoff Salmon, Giambattista Parascandolo, Gildas Chabot, Grace Zhao, Greg Brockman, Guillaume Leclerc, Hadi Salman, Haiming Bao, Hao Sheng, Hart Andrin, Hessam Bagherinezhad, Hongyu Ren, Hunter Lightman, Hyung Won Chung, Ian Kivlichan, Ian O’Connell, Ian Osband, Ignasi Clavera Gilaberte, Ilge Akkaya, Ilya Kostrikov, Ilya Sutskever, Irina Kofman, Jakub Pachocki, James Lennon, Jason Wei, Jean Harb, Jerry Twore, Jiacheng Feng, Jiahui Yu, Jiayi Weng, Jie Tang, Jieqi Yu, Joaquin Quiñonero Candela, Joe Palermo, Joel Parish, Johannes Heidecke, John Hallman, John Rizzo, Jonathan Gordon, Jonathan Uesato, Jonathan Ward, Joost Huizinga, Julie Wang, Kai Chen, Kai Xiao, Karan Singh, Karina Nguyen, Karl Cobbe, Katy Shi, Kayla Wood, Kendra Rimbach, Keren Gu-Lemberg, Kevin Liu, Kevin Lu, Kevin Stone, Kevin Yu, Lama Ahmad, Lauren Yang, Leo Liu, Leon Maksin, Leyton Ho, Liam Fedus, Lilian Weng, Linden Li, Lindsay McCallum, Lindsey Held, Lorenz Kuhn, Lukas Kondraciuk, Lukasz Kaiser, Luke Metz, Madelaine Boyd, Maja Trebacz, Manas Joglekar, Mark Chen, Marko Tintor, Mason Meyer, Matt Jones, Matt Kaufer, Max Schwarzer, Meghan Shah, Mehmet Yatbaz, Melody Y. Guan, Mengyuan Xu, Mengyuan Yan, Mia Glaese, Mianna Chen, Michael Lampe, Michael Malek, Michele Wang, Michelle Fradin, Mike McClay, Mikhail Pavlov, Miles Wang, Mingxuan Wang, Mira Murati, Mo Bavarian, Mostafa Rohaninejad, Nat McAleese, Neil Chowdhury, Neil Chowdhury, Nick Ryder, Nikolas Tezak, Noam Brown, Ofir Nachum, Oleg Boiko, Oleg Murk, Olivia Watkins, Patrick Chao, Paul Ashbourne, Pavel Izmailov, Peter Zhokhov, Rachel Dias, Rahul Arora, Randall Lin, Rapha Gontijo Lopes, Raz Gaon, Reah Miyara, Reimar Leike, Renny Hwang, Rhythm Garg, Robin Brown, Roshan James, Rui Shu, Ryan Cheu, Ryan Greene, Saachi Jain, Sam Altman, Sam Toizer, Sam Toyer, Samuel Miserendino, Sandhini Agarwal, Santiago Hernandez, Sasha Baker, Scott McKinney, Scottie Yan, Shengjia Zhao, Shengli Hu, Shibani Santurkar, Shraman Ray Chaudhuri, Shuyuan Zhang, Siyuan Fu, Spencer Papay, Steph Lin, Suchir Balaji, Suvansh Sanjeev, Szymon Sidor, Tal Broda, Aidan Clark, Tao Wang, Taylor Gordon, Ted Sanders, Tejal Patwardhan, Thibault Sottiaux, Thomas Degry, Thomas Dimson, Tianhao Zheng, Timur Garipov, Tom Stasi, Trapit Bansal, Trevor Creech, Troy Peterson, Tyna Eloundou, Valerie Qi, Vineet Kosaraju, Vinnie Monaco,

Vitchyr Pong, Vlad Fomenko, Weiyi Zheng, Wenda Zhou, Wes McCabe, Wojciech Zaremba, Yann Dubois, Yinghai Lu, Yiming Chen, Young Cha, Yu Bai, Yuchen He, Yuchen Zhang, Yunyun Wang, Zheng Shao, and Zhuohan Li. Openai o1 system card, 2024. <https://arxiv.org/abs/2412.16720>.

Long Ouyang, Jeffrey Wu, Xu Jiang, Diogo Almeida, Carroll Wainwright, Pamela Mishkin, Chong Zhang, Sandhini Agarwal, Katarina Slama, Alex Ray, et al. Training language models to follow instructions with human feedback. *Advances in neural information processing systems*, 35:27730–27744, 2022.

Nicolas Le Roux, Marc G Bellemare, Jonathan Lebensold, Arnaud Bergeron, Joshua Greaves, Alex Fréchette, Carolyne Pelletier, Eric Thibodeau-Laufer, Sándor Toth, and Sam Work. Tapered off-policy reinforce: Stable and efficient reinforcement learning for llms. *arXiv preprint arXiv:2503.14286*, 2025.

John Schulman, Sergey Levine, Pieter Abbeel, Michael Jordan, and Philipp Moritz. Trust region policy optimization. In *International conference on machine learning*, pages 1889–1897. PMLR, 2015.

John Schulman, Filip Wolski, Prafulla Dhariwal, Alec Radford, and Oleg Klimov. Proximal policy optimization algorithms. *arXiv preprint arXiv:1707.06347*, 2017.

Zhihong Shao, Peiyi Wang, Qihao Zhu, Runxin Xu, Junxiao Song, Xiao Bi, Haowei Zhang, Mingchuan Zhang, YK Li, Y Wu, et al. Deepseekmath: Pushing the limits of mathematical reasoning in open language models. *arXiv preprint arXiv:2402.03300*, 2024.

Guangming Sheng, Chi Zhang, Zilingfeng Ye, Xibin Wu, Wang Zhang, Ru Zhang, Yanghua Peng, Haibin Lin, and Chuan Wu. Hybridflow: A flexible and efficient rlhf framework. *arXiv preprint arXiv: 2409.19256*, 2024.

Zhenpeng Su, Leiyu Pan, Xue Bai, Dening Liu, Guanting Dong, Jiaming Huang, Wenping Hu, and Guorui Zhou. Klear-reasoner: Advancing reasoning capability via gradient-preserving clipping policy optimization. *arXiv preprint arXiv:2508.07629*, 2025.

Kimi Team, Angang Du, Bofei Gao, Bowei Xing, Changjiu Jiang, Cheng Chen, Cheng Li, Chenjun Xiao, Chenzhuang Du, Chonghua Liao, et al. Kimi k1. 5: Scaling reinforcement learning with llms. *arXiv preprint arXiv:2501.12599*, 2025.

Shenzi Wang, Le Yu, Chang Gao, Chujie Zheng, Shixuan Liu, Rui Lu, Kai Dang, Xionghui Chen, Jianxin Yang, Zhenru Zhang, et al. Beyond the 80/20 rule: High-entropy minority tokens drive effective reinforcement learning for llm reasoning. *arXiv preprint arXiv:2506.01939*, 2025a.

Yiping Wang, Qing Yang, Zhiyuan Zeng, Liliang Ren, Lucas Liu, Baolin Peng, Hao Cheng, Xuehai He, Kuan Wang, Jianfeng Gao, et al. Reinforcement learning for reasoning in large language models with one training example. *arXiv preprint arXiv:2504.20571*, 2025b.

Wei Xiong, Jiarui Yao, Yuhui Xu, Bo Pang, Lei Wang, Doyen Sahoo, Junnan Li, Nan Jiang, Tong Zhang, Caiming Xiong, et al. A minimalist approach to llm reasoning: from rejection sampling to reinforce. *arXiv preprint arXiv:2504.11343*, 2025.

An Yang, Beichen Zhang, Binyuan Hui, Bofei Gao, Bowen Yu, Chengpeng Li, Dayiheng Liu, Jianhong Tu, Jingren Zhou, Junyang Lin, et al. Qwen2. 5-math technical report: Toward mathematical expert model via self-improvement. *arXiv preprint arXiv:2409.12122*, 2024.

An Yang, Anfeng Li, Baosong Yang, Beichen Zhang, Binyuan Hui, Bo Zheng, Bowen Yu, Chang Gao, Chengan Huang, Chenxu Lv, et al. Qwen3 technical report. *arXiv preprint arXiv:2505.09388*, 2025.

Qiyi Yu, Zheng Zhang, Ruofei Zhu, Yufeng Yuan, Xiaochen Zuo, Yu Yue, Tiantian Fan, Gaohong Liu, Lingjun Liu, Xin Liu, et al. Dapo: An open-source llm reinforcement learning system at scale. *arXiv preprint arXiv:2503.14476*, 2025.

Yufeng Yuan, Qiyi Yu, Xiaochen Zuo, Ruofei Zhu, Wenyuan Xu, Jiaze Chen, Chengyi Wang, TianTian Fan, Zhengyin Du, Xiangpeng Wei, et al. Vapo: Efficient and reliable reinforcement learning for advanced reasoning tasks. *arXiv preprint arXiv:2504.05118*, 2025a.

Yufeng Yuan, Yu Yue, Ruofei Zhu, Tiantian Fan, and Lin Yan. What's behind ppo's collapse in long-cot? value optimization holds the secret. *arXiv preprint arXiv:2503.01491*, 2025b.

Xiaojiang Zhang, Jinghui Wang, Zifei Cheng, Wenhao Zhuang, Zheng Lin, Minglei Zhang, Shaojie Wang, Yinghan Cui, Chao Wang, Junyi Peng, Shimiao Jiang, Shiqi Kuang, Shouyu Yin, Chaohang Wen, Haotian Zhang, Bin Chen, and Bing Yu. Srpo: A cross-domain implementation of large-scale reinforcement learning on llm, 2025. <https://arxiv.org/abs/2504.14286>.

Xiaotian Zhang, Chunyang Li, Yi Zong, Zhengyu Ying, Liang He, and Xipeng Qiu. Evaluating the performance of large language models on gaokao benchmark. *arXiv preprint arXiv:2305.12474*, 2023.

Yanli Zhao, Andrew Gu, Rohan Varma, Liang Luo, Chien-Chin Huang, Min Xu, Less Wright, Hamid Shojanazeri, Myle Ott, Sam Shleifer, et al. Pytorch fsdp: experiences on scaling fully sharded data parallel. *arXiv preprint arXiv:2304.11277*, 2023.

Chujie Zheng, Shixuan Liu, Mingze Li, Xiong-Hui Chen, Bowen Yu, Chang Gao, Kai Dang, Yuqiong Liu, Rui Men, An Yang, et al. Group sequence policy optimization. *arXiv preprint arXiv:2507.18071*, 2025a.

Haizhong Zheng, Yang Zhou, Brian R Bartoldson, Bhavya Kailkhura, Fan Lai, Jiawei Zhao, and Beidi Chen. Act only when it pays: Efficient reinforcement learning for llm reasoning via selective rollouts. *arXiv preprint arXiv:2506.02177*, 2025b.

Yinmin Zhong, Zili Zhang, Xiaoniu Song, Hanpeng Hu, Chao Jin, Bingyang Wu, Nuo Chen, Yukun Chen, Yu Zhou, Changyi Wan, et al. Streamrl: Scalable, heterogeneous, and elastic rl for llms with disaggregated stream generation. *arXiv preprint arXiv:2504.15930*, 2025.

Zilin Zhu, Chengxing Xie, Xin Lv, and slime Contributors. slime: An llm post-training framework for rl scaling. <https://github.com/THUDM/slime>, 2025. GitHub repository. Corresponding author: Xin Lv.

Appendix

Acknowledgment

We would like to thank Cheng Luo, Xinyu Yang, Ranajoy Sadhukhan, Xuesheng Liu, Yongji Wu for providing us constructive feedback on our paper and the computing resources of NVIDIA. This work is supported in part by the grants NSF CCF-2504353 to B. Chen. This work is also partially supported by Google Research Award, Amazon Research Award, Intel, Li Auto, Moffett AI, and CMU CyLab Seed funding. We are also grateful to BitDeer AI Research for providing GPU resources. Any opinions, findings, and conclusions or recommendations expressed are those of the authors and do not necessarily reflect the views of the National Science Foundation.

Ethics Statement

This work focuses on developing reinforcement learning algorithms for large language models. Our research does not involve human subjects, personally identifiable information, or sensitive data. All datasets used are publicly available and widely adopted in the community. We acknowledge that more capable LLMs may have potential societal impacts, including misuse for generating misleading or harmful content. To mitigate these risks, our study is confined to controlled academic settings, and our primary goal is to improve the stability and efficiency of training methods.

The Use of Large Language Models (LLMs)

We used large language models (LLMs) as general-purpose assistants in two limited ways: (1) for writing polish, including improving grammar, readability, and presentation of the manuscript, and (2) as code assistants (e.g., Cursor, GitHub Copilot) to accelerate routine coding tasks such as debugging syntax errors and refactoring simple functions. LLMs were not used for research ideation, algorithm design, experimental analysis, or drawing conclusions. All conceptual and scientific contributions are entirely the work of the authors.

A Overview

In this appendix, we provide additional details to complement the main text. Appendix B describes the experimental setup in full, including datasets, models, and training hyperparameters. Appendix C presents theoretical proofs supporting our method and analysis. Appendix D includes additional experimental results.

B Detailed Experimental Setting

Models & Datasets. To verify the effectiveness of our method, we extensively evaluate M2PO on six models from four model series: Qwen2.5-Math-7B (Yang et al., 2024), Llama-3.2-3B-Instruct (Dubey et al., 2024), Qwen3-Base-1.7B/4B/8B (Yang et al., 2025), and Qwen2.5-32B (Yang et al., 2024). For Qwen2.5-Math-7B, we use a context length of 4k, which is the maximum for this series. while for all other models the context length is set to 16k. For training, we adopt the DeepScaleR (Luo et al., 2025b) math dataset.

Training. Our method is implemented based on verl (Sheng et al., 2024) pipeline and uses vLLM (Kwon et al., 2023) for rollout. We use a mix of H100 and H200 servers for training, depending on resource availability. We set the rollout temperature to 1 for vLLM (Kwon et al., 2023). The training batch size is set to 256, and the mini-batch size to 512. We sample 8 responses per prompt. We train all models for 1000 steps, and we optimize the actor model using the AdamW (Loshchilov and Hutter, 2019) optimizer with a constant learning rate of 1e-6. We use $\beta_1 = 0.9$, $\beta_2 = 0.999$, and apply a weight decay of 0.01. We use the following question template to prompt the LLM. For reward assignment, we give a score of 0.1 for successfully extracting an answer and a score of 1.0 if the extracted answer is correct. Similar to (Yu et al., 2025), we remove the KL-divergence term. The optimization is performed on the parameters of the actor module wrapped with Fully Sharded Data Parallel (FSDP) (Zhao et al., 2023) for efficient distributed training. We set the M2PO threshold to 0.04 for all training runs.

Evaluation. For benchmark datasets, we use eight widely used complex mathematical reasoning benchmarks to evaluate the performance of trained models: Math500 (Hendrycks et al., 2021; Lightman et al., 2023), AIME24/25 (Art of Problem Solving, 2024a), AMC23/24 (Art of Problem Solving, 2024b), Minerva Math (Lewkowycz et al., 2022), Gaokao (Zhang et al., 2023), Olympiad Bench (He et al., 2024). Same as the training setting, For Qwen2.5-Math-7B models, we use 4k as the context length. For other models, we set the context length to 16k. Similar to (Wang et al., 2025b; Zheng et al., 2025b), we evaluate models on those benchmarks every 50 steps and report the performance of the checkpoint that obtains the best average performance on eight benchmarks. We evaluate all models with temperature = 1. For AIME24/25, we report the *pass@1*(*avg@16*), for other benchmarks, we report the *pass@1*(*avg@4*).

Question Template

Please solve the following math problem: {{Question Description}}. The assistant first thinks about the reasoning process step by step and then provides the user with the answer. Return the final answer in \boxed{} tags, for example \boxed{1}. Let's solve this step by step.

C Theoretical Proof

Proof of Theorem 5.1.

Proof. Let $z = \log r$, so that $r = e^z$. Since $1/R < r \leq R$, we have $|z| \leq \log R$.

For $z \geq 0$, observe that

$$\frac{e^z - 1}{z} = \int_0^1 e^{tz} dt \leq \int_0^1 e^z dt = e^z,$$

which implies $(e^z - 1)^2 \leq (ze^z)^2 = z^2 e^{2z}$.

For $z \leq 0$, set $u = -z \geq 0$. Then

$$(e^z - 1)^2 = (1 - e^{-u})^2 \leq u^2 = z^2 \leq z^2 e^{2|z|}.$$

Combining both cases, for all $z \in \mathbb{R}$ we obtain

$$(e^z - 1)^2 \leq z^2 e^{2|z|}.$$

Substituting $Z = \log r$, this yields

$$(r-1)^2 \leq (\log r)^2 e^{2|\log r|} \leq R^2 (\log r)^2.$$

Taking expectation under π_{behav} gives

$$\chi^2(\pi_{\text{new}} \parallel \pi_{\text{behav}}) = \mathbb{E}_{\pi_{\text{behav}}} [(r-1)^2] \leq R^2 \mathbb{E}_{\pi_{\text{behav}}} [(\log r)^2] = R^2 M_2.$$

□

D Additional Experiments

Commonly clipped tokens in GRPO. Figure 10 shows the specific tokens that are most frequently clipped by ϵ -clipping. The word cloud of commonly clipped tokens is highly aligned with high-entropy tokens shown in (Wang et al., 2025a): these tokens are not random or unimportant, but rather belong to the most semantically and structurally critical elements in reasoning traces. Many of them (e.g., First, simplify, determine, To def, Thus, verify, break) are precisely the high-entropy “pivotal tokens” that initiate, connect, or conclude key reasoning steps. Others (e.g., assistant, user, code markers like ### or \$\$) serve as structural anchors in the dialogue or mathematical formatting. This observation aligns with Figure 4b: as the importance weight ratio $|r-1|$ grows, clipped tokens tend to exhibit higher entropy.

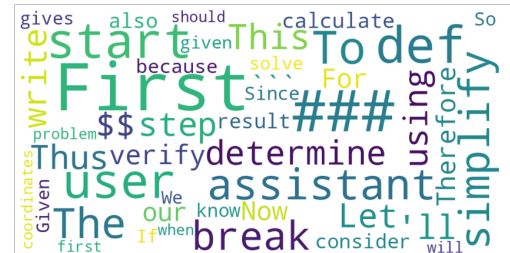


Figure 10 Word clouds of frequently clipped tokens with ϵ clipping.

M2PO under different staleness. In Table 1, we compare the performance between M2PO and other baselines under $s=256$. To further study the robustness of M2PO across different staleness levels, we train Qwen2.5-Math-7B with M2PO under $s=0, 32, 64, 128, 256$, as shown in Figure 11. We observe that larger staleness slightly slows down the initial accuracy gain during the very early phase of training, reflecting the expected delay when using outdated rollouts. However, this effect quickly diminishes: all curves steadily improve and converge to nearly the same accuracy. Notably, even under extreme staleness ($s=256$), M2PO achieves performance on par with the on-policy case ($s=0$), without signs of collapse or degradation. These results highlight that M2PO effectively preserves the learning signal contained in stale data, enabling stable training and strong generalization across a wide range of staleness values.

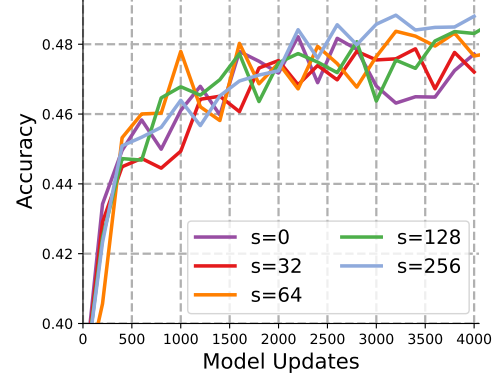


Figure 11 The performance of M2PO under different staleness on Qwen2.5-Math-7B.